Catalysis Today 419 (2023) 114160

Contents lists available at ScienceDirect

Catalysis Today

journal homepage: www.elsevier.com/locate/cattod

P-Doped carbon catalyst highly efficient for benzodiazepine synthesis. Tires valorisation

Marina Godino-Ojer [a], Vanessa Ripoll Morales [a], Antonio J. López Peinado [b], Maria Bernardo [c], Nuno Lapa [c], Ana Maria Ferraria [d,e], Ana Maria Botelho do Rego [d,e], Isabel M. Fonseca [c], Ines Matos [c,*], Elena Pérez-Mayoral [b,*]

[a] Facultad de Ciencias Experimentales, Universidad Francisco de Vitoria, UFV, Ctra. Pozuelo-Majadahonda km 1.800, 28223 Pozuelo de Alarcón, Madrid, Spain
[b] Departamento de Química Inorgánica y Química Técnica, Universidad Nacional de Educación a Distancia, UNED, Facultad de Ciencias, Urbanización Monte Rozas, Avda. Esparta s/n Ctra. de Las Rozas al Escorial Km 5, 528232 Las Rozas, Madrid, Spain
[c] LAQV/REQUIMTE, Departamento de Química, Faculdade de Ciências e Tecnologia, Universidade Nova de Lisboa, 2829-516 Caparica, Portugal
[d] BSIRG, IBB - Institute for Bioengineering and Biosciences, Departamento de Engenharia Química, Instituto Superior Técnico, Universidade de Lisboa, 1049-001 Lisboa, Portugal
[e] Associate Laboratory i4HB—Institute for Health and Bioeconomy at Instituto Superior Técnico, Universidade de Lisboa, Av. Rovisco Pais, 1049-001 Lisboa, Portugal

ARTICLE INFO

Keywords:
Carbon materials
Heterogeneous catalysis, Fine chemicals
Waste valorization

ABSTRACT

Carbon catalysts prepared from pyrolysis of spent tires are found to efficiently catalyse the synthesis of benzodiazepine **1**, from *o*-phenylendiamine **2** and acetone **3**, with high conversions and selectivity, under mild reaction conditions, according to Scheme 1.

The most acidic catalyst, CPN_H_3PO_4, obtained by chemical activation with H_3PO_4, resulted on the most efficient catalyst affording conversion values higher than 90 %, after 4 h of reaction time, and selectively leading to benzodiazepine **1** (90 %). On the other hand, the CPN and CPN_CO_2 catalysts reached high conversions of **2** although diminished selectivity to **1**, confirming that the carbon matrix is involved in the first steps of the reaction mainly catalyzing the formation of intermediate **4** as the main reaction product.

Note that all the investigated catalysts are macroporous materials with pore size distribution large enough to favor diffusion of reactants and products. Therefore, the catalytic performance is mainly governed by the chemical surface, in particular by the presence of acid functions as phosphate groups anchored to the carbon surface or as SiP_2O_7 supported phase.

Finally, considering both experimental and theoretical results, it seems that the most probable catalytic centers comprise phosphate functions in SiP_2O_7 catalyzing the last cyclization step to **1**. Although electrophilicity of carbon acceptor (C═N moiety) in the presence of model simulating phosphate groups anchored to the carbon surface was slightly superior, transition structure in the presence of model simulating SiP_2O_7 showed the smallest free energy barrier.

1. Introduction

Spent tires constitute a serious environmental problem worldwide. Automobiles are an important part of the transportation system and although used tires are often reused, effective technology for their recycling has not yet been developed. Properties of the material for its manufacture including great durability and low biological degradation, make both the management and disposal of this waste very expensive. Tire industry in Europe but also to international level is working by designing tires with optimal performance and durability. This industry also applies the circular economy, retreading being a practical example of resource efficiency [1]. In this context, spent tires are important resources useful for construction, automotive, cement industries, among others, betting on valorising this waste.

High carbon content of this type of waste makes feasible to transform them into valuable compounds such as activated carbons (ACs). Processing parameters in particular temperature and heating rate on the pyrolysis greatly influence the final characteristic of the material [2].

* Corresponding authors.
E-mail addresses: Ines.matos@fct.unl.pt (I. Matos), eperez@ccia.uned.es (E. Pérez-Mayoral).

https://doi.org/10.1016/j.cattod.2023.114160
Received 29 December 2022; Received in revised form 27 March 2023; Accepted 18 April 2023
Available online 20 April 2023

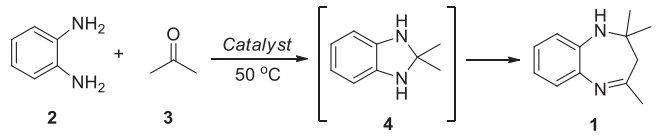

Scheme 1. Synthesis of 2,2,4-trimethyl-2,3-dihydro-1*H*-1,5-benzodiazepine **1** from *o*-phenylendiamine **2** and acetone **3**, at 50 °C, under solvent-free conditions.

Over the last years, ACs from tires have gained importance in several environmental applications as adsorbents [3] including the organic contaminants removal [4,5] or NOx control [6], among others. However, as far as we know this type of ACs have never been used in fine chemical synthesis.

The goal of this paper is to synthesise and characterise a new family of carbonaceous materials, prepared from used tires, able to efficiently catalyse the synthesis of benzodiazepines, from the corresponding *o*-phenylendiamines and acetone (Schemes 1 and 2).

Benzodiazepines are one of the most pharmacologically relevant nitrogenous heterocycles showing a great variety of biological activities – anti-inflammatory, antiviral, analgesic, sedative, hypnotic, antidepressive, anti-HIV etc – [7]. Specifically, 1,5-benzodiazepines consist of a seven-membered ring fused to a benzene ring in which two nitrogen atoms are located at 1- and 5- positions often applied as anxiolytic and anti-convulsive drugs [8].

Several structurally different porous catalysts applied to the synthesis of 1,5-benzodiazepines by using different synthetic approaches –zeolites, silica supported catalysts, graphene oxide, silica, clay, magnesium oxide and iron oxide *etc.* –have been reported [9]. At this regard, we recently reported the first examples of carbon supported zirconia or sulfated zirconia efficiently catalysing the synthesis of 2,2,4-trimethyl-2,3-dihydro-1*H*-1,5-benzodiazepine **1** (Scheme 1), even much more active and selective than zeolites or mesoporous silica catalysts. In this case, -OSO_3H functional groups over the zirconia or carbon surfaces seem to be responsible of the increased selectivity to the corresponding benzodiazepine [9]. In addition, authors demonstrated that carbon matrix is involved in the reaction, making these materials environmental-friendly and effective alternative catalysts. Based on that, much more recently we reported a new study concerning to the synthesis of 2,2,4-trimethyl-2,3-dihydro-1*H*-1,5-benzodiazepine **1** in the presence of acidic carbon catalysts showing different structures, morphologies, and compositions, under mild conditions. Both acidity and porosity of the catalysts were key on conversion and selectivity [11].

In this work, we seek to develop a novel series of carbon-based catalysts prepared from used tires submitted to pyrolysis treatment followed by activation or not with H_3PO_4 or CO_2 and applied to the synthesis of 2,2,4-trimethyl-2,3-dihydro-1*H*-1,5-benzodiazepine **1** and related compounds **5** and **6** from the corresponding *o*-phenylendiamine and acetone **3**, under mild conditions, according to Schemes 1 and 2.

It is known from the literature and our previous work [12–15] that activation with phosphoric acid results not only in the development of porosity but also introduces phosphorus groups in the surface of the material. Thus, in a single step it is possible to obtain functionalization of the surface without the need to any further treatment. These phosphorus groups are very stable and confer acidity to the carbon surface. On the other hand, thermal treatment under CO_2 atmosphere is well known to develop microporosity on the carbon material. Additionally, this treatment increases the basic character of the porous carbon due to the preponderance of the basal plane chemistry [16]. Thus, in this work three different porous materials derived from spent tire rubber will be study. Complementarily, in order to find the most probable catalytic active specie in the most efficient catalyst, we analysed the transition structures of the cyclization final step by computational methods by using the most probable and reduced models simulating the catalytic sites.

2. Materials and methods

2.1. Synthesis of the catalysts

Used tire rubber was collected in a Portuguese mechanical recycling facility and used as raw material which will be pyrolyzed. It was ground and sieved to a 2–4 mm particle size.

Materials under study were synthesized by tire pyrolysis followed by activation, or not, with H_3PO_4 or CO_2.

2.1.1. Pyrolysis conditions

Pyrolysis of the rubber were carried out according to the experimental protocol previously reported [5]. Briefly, pyrolysis of spent tire rubber was carried out in a 5.5 dm^3 stirred batch reactor (Parr Instruments, Hastelloy C276, Illinois, USA) which was purged and pressurized to 0.6 MPa with N_2 flow by heating (room temperature to 405 °C at 5 C° min^{-1} and keeping the final temperature during 30 min). After cooling to room temperature, the char was separated from the liquid fraction by settling and extracted with hexane. The char obtained was named as CPN.

2.1.2. Activated samples

The obtained CPN char was subjected to a physical activation with CO_2 and a chemical activation with H_3PO_4 as activating agents. The activated char CPN_CO_2 was obtained through physical activation performed in a quartz reactor placed in an electric vertical tube furnace. First the sample was heated with a heating rate of 10 °C.min^{-1}. until 500 ºC and kept at that temperature for 1 h then it was raised until at 800 °C and kept for 3 h, under a 100 mL·min^{-1} flow of CO_2.

The chemical activation starts with the impregnation of the char with H_3PO_4 using a mass ratio of 1:1, at 50 °C, for 5 h, followed by drying at 130 °C. The impregnated char is subject to a thermal treatment at 500 °C for 2 h with a heating rate of 5 °C.min^{-1}, always under an N_2 flow of 150 mL·min^{-1}. After cooling under N_2 flow, the samples were thoroughly washed with deionized water until constant pH value was reached (pH of deionized water). The obtained catalyst was named

Table 1
Elemental analysis (% w/w), and pH_{PZC} of ST rubber and carbons.

Catalyst	Ash	C	H	N	S	pH_{PZC}
ST rubber[a]	2.96	86.8	7.36	0.00	1.23	n.d.
CPN	12.9	86.7	0.83	0.00	2.67	6.80
CPN_CO_2	24.1	82.52	0.16	0.51	2.53	7.6
CPN_H_3PO_4	21.3	87.76	0.39	0.49	0.62	2.8

[a] As-received basis; n.d. – not determined

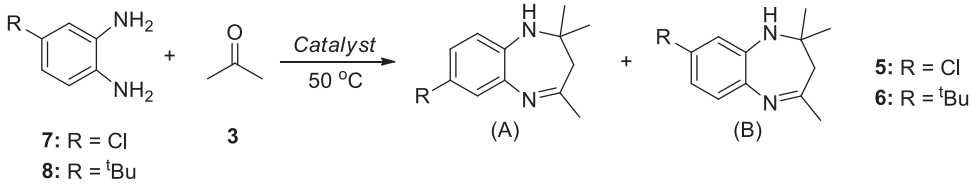

Scheme 2. Synthesis of benzodiazepines **5** and **6** from 4-substituted *o*-phenylendiamines **7** and **8** and acetone **3**, at 50 °C, under solvent-free conditions.

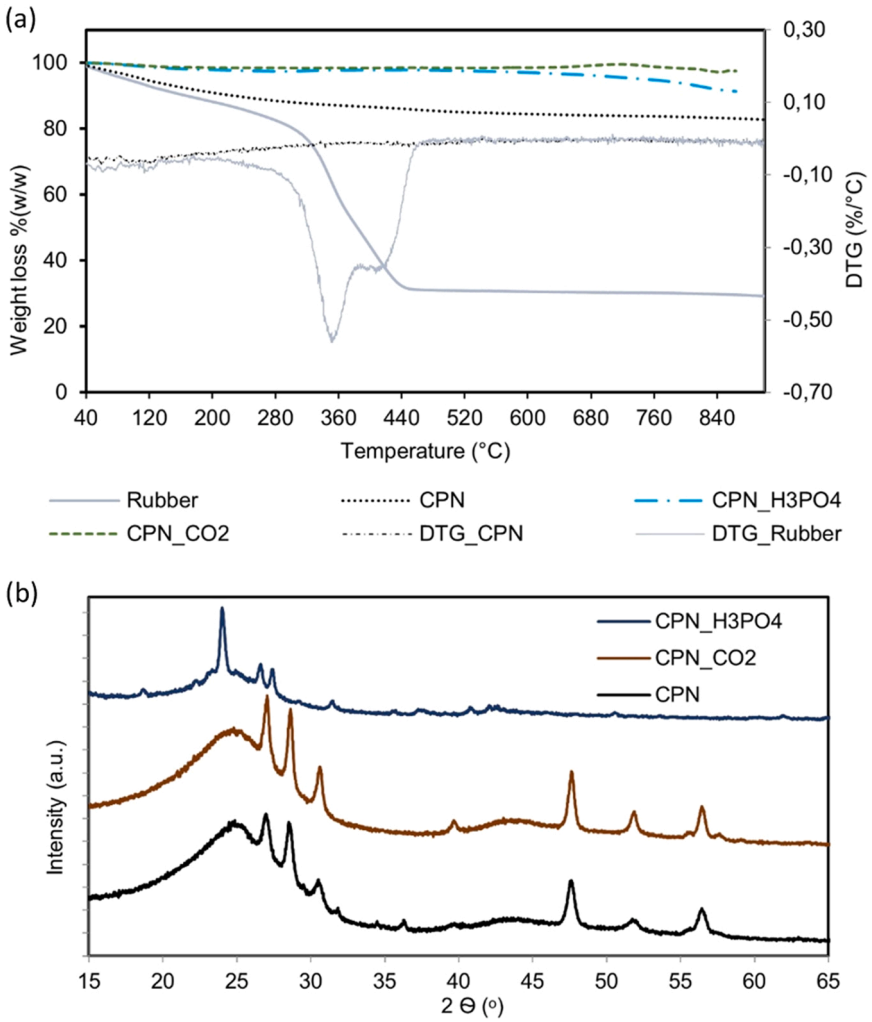

Fig. 1. (a) TGA curves and (b) XRD patterns of ST rubber, char sample and ACs.

CPN_H_3PO_4.

2.2. Characterization of the catalysts

The catalyst samples prepared for this research work were characterized by determining (i) elemental analysis, (ii) thermogravimetric analysis (TGA), (iii) N_2 adsorption-desorption isotherms at 77 K, (iv) pH at the point of zero-charge (pH_{PZC}), (v) X-ray powder diffraction (XRPD), (vi) ash content, and (vii) Fourier-transform infrared spectroscopy (FTIR),

Elemental analysis, CNHS quantification was performed in a Thermo Finnigan-CE Instruments Flash EA 1112 CHNS analyzer, following the standards ASTM D5373 (C, H, N) and ASTM D4239 (S).

Thermogravimetric analysis, TGA was performed in a Setaram Labsys instrument, EVO model, with a 20 $cm^3.min^{-1}$ Argon flow and a heating rate of 5 °C·min^{-1} up to 900 ºC.

Textural analysis, N_2 adsorption-desorption isotherms at −196 °C were acquired on an ASAP 2010 V1.01 B Micromeritics equipment and the following parameters determined: Apparent surface area (S_{BET}) by using Brunauer–Emmett–Teller (BET) equation; Total pore volume (V_{total}) determined by the amount of nitrogen adsorbed at the relative pressure $P/P^0 = 0.99$; Micropore volume (V_{micro}) using the *t*-plot method; and Mesopore volume (V_{meso}) by the difference between V_{total} and V_{micro}.

pH_{PZC}, determination of the pH at the point of zero-charge followed the point drift procedure described in [17].

X-ray powder diffraction, XRPD diffractograms were acquired using a benchtop x-ray diffractometer (RIGAKU, model MiniFlex II, USA), with a Cu X-ray tube (30 kV/15 mA) by continuous scanning from 15º to 80º (2θ) with a step size of 0.01º (2θ) and a scan speed of 2º.min^{-1}.

FTIR spectra were acquired using a Cary 630 FTIR spectrometer (Agilent Technologies) equipped with diamond attenuated reflectance (ATR) over the range of 400–4000 cm^{-1}, at room temperature, with a resolution of 1 cm^{-1}.

XPS analysis was performed using a XSAM800 non-monochromatic dual anode spectrometer from Kratos. Spectra were obtained using the Mg Kα X–ray source (1253.6 eV). Samples were analyzed, compacting the powder on a double sided tape, at room temperature (~20 °C), setting a take-off angle of 45° and under a pressure around 10^{-7} Pa. Peak-fitting, using Shirley backgrounds and pseudo-Voigt profiles (Gaussian-Lorentzian products), was performed using XPSPEAK4.1. For quantification purposes, the sensitivity factors (SF) were furnished by the library from software Vision 2 for Windows, Version 2.2.9 from KRATOS: 0.318 for C 1 s, 0.736 for O 1 s, 0.723 for S 2p, 0.371 for Si 2p, 0.505 for N 1 s, 0.53 for P 2p and 3.21 for Zn $2p_{3/2}$.

2.3. Catalytic performance

To a mixture of the corresponding *o*-phenylendiamine (1 mmol) and acetone **3** (10 mmol) in a three-necked vessel, equipped with reflux condenser, septum and thermometer, placed on a multi-experiment workstation StarFish (Radleyś Discovery Technologies IUK), at 50 °C,

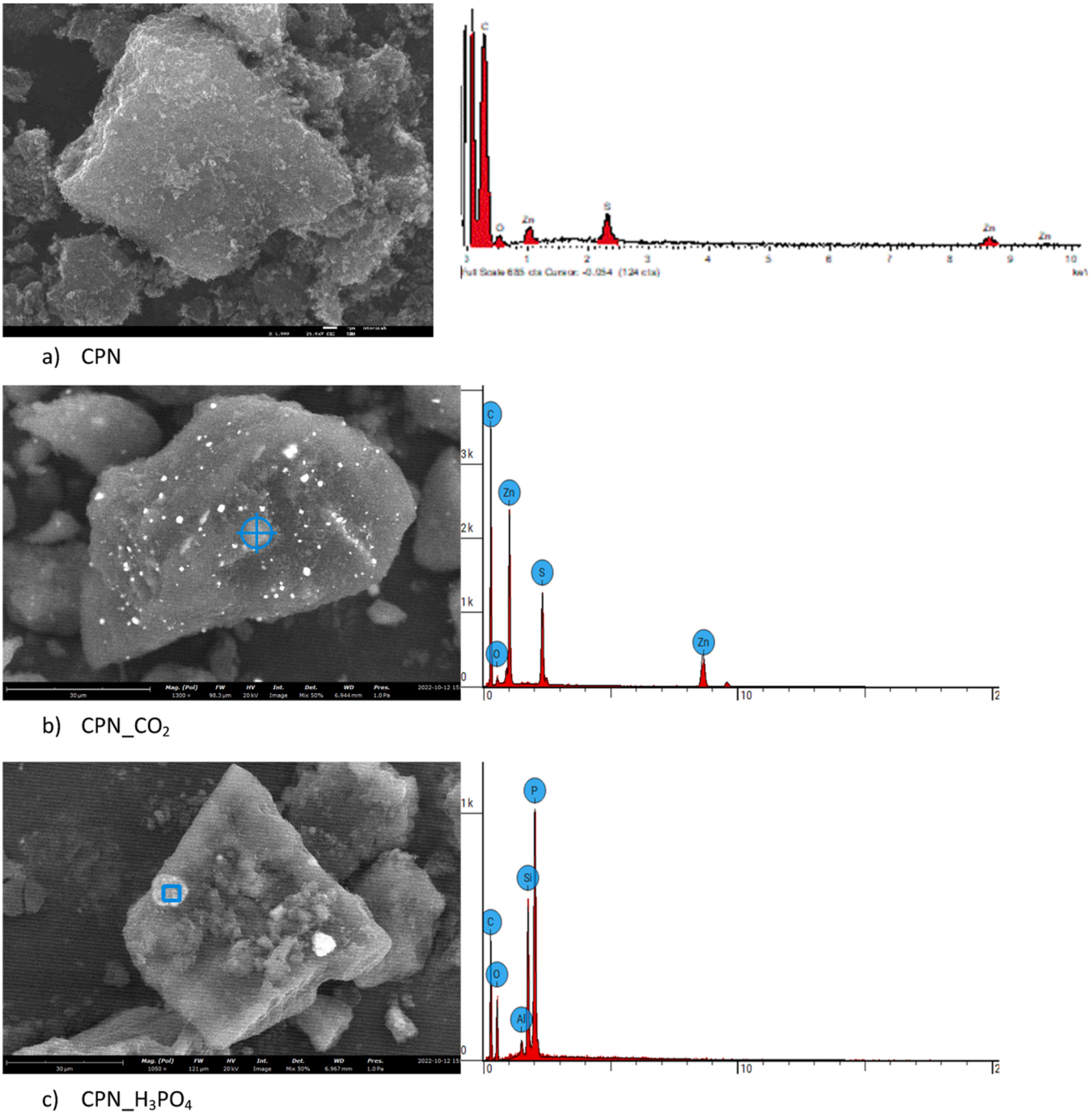

Fig. 2. SEM images of the catalysts CPN, CPN_CO_2, CPN_H_3PO_4 and respective EDS.

Table 2a
Atomic concentrations (%) of relevant elements in carbon samples.

	CPN	CPN_CO_2	CPN_H_3PO_4
C	90.9	93.1	83.5
O	6.59	5.46	13.6
S	0.79	0.65	0.14
Si	n.q.	n.q.	0.24
Zn	0.96	0.75	0.09
P	–	–	2.04
N	0.74	n.q.	0.51

Abbreviation: n.q.: not quantifiable

the catalyst was added (50 mg) and the reaction mixture was stirred during 240 min. The samples were periodically collected at 15, 30, 60, 120, 180 and 240 min, diluted with acetone (0.5 mL), and the catalyst was filtered off and the solvent evaporated in vacuum.

The catalysts were milled and sieved to particle size < 0.250 mm, in order to avoid mass transfer limitations. reaction progress was qualitatively followed by TLC chromatography performed on DC-Aulofolien/Kieselgel 60 F245 (Merk) using mixtures of CH_2Cl_2/EtOH (98:2) as eluent.

Conversion is defined as the fraction of the corresponding *o*-phenylendiamine transformed at each reaction time into compounds determined by ^{1}H NMR.

The reaction products were characterized by ^{1}H NMR spectroscopy.

Table 2b
Peak positions (eV), atomic concentrations (%) and assignments for the XPS detailed regions.

	CPN		CPN_CO_2		CPN_H_3PO_4		Assignments
	BE (eV)	at. %	BE (eV)	at. %	BE (eV)	at. %	
C 1s 1	284.9	68.0	284.9	70.0	284.9	62.5	C-C, C-H, C-S, C-N, C-O
C 1s 2	285.8	14.6	286.3	12.6	286.1	8.8	Epoxides and/or C-O-PO_3H_2 for sample CPN_H_3PO_4
C 1s 3	287.0	4.7	287.5	6.0	287.2	5.7	
C 1s 4	288.2	2.0	288.9	2.5	288.6	3.2	C═O, O-C═O^-
C 1s 5	289.6	1.6	290.1	2.0	290.0	2.3	-COOH
C 1s 6	291.2		291.4		291.3		π→π *
C 1s 7					292.5		
O 1s 1			531.1	0.54	531.5	3.9	C═O and/or C-O-PO_3H_2 for sample CPN_H_3PO_4
O 1s 2	533.1	6.6	533.2	4.0	533.0	7.1	C-O; SiP_2O_7,
O 1s 3			535.4	0.88	534.5	1.8	H_2O
O 1s 4					536.4	0.57	aggregated H_2O
S $2p_{3/2}$ 1	162.7	0.42	162.8	0.19			S^{2-}
S $2p_{1/2}$ 1	163.9	0.21	164.0	0.09			
S $2p_{3/2}$ 2	164.4	0.11	164.4	0.24	164.4	0.10	Thiol
S $2p_{1/2}$ 2	165.6	0.06	165.6	0.12	165.6	0.05	
Zn $2p_{3/2}$	1022.4	1.0	1022.5	0.75	1022.3	0.09	Zn^{2+}
N 1s 1	399.0	0.31			399.2	0.13	C-N
N 1s 2	400.9	0.44			401.6	0.37	$C-N^+$
P $2p_{3/2}$ 1					134.0	1.20	C-O-PO_3H_2
P $2p_{1/2}$ 1					134.9	0.60	
P $2p_{3/2}$ 2					134.6	0.16	SiP_2O_7
P $2p_{1/2}$ 2					135.8	0.08	
Si $2p_{3/2}$					104.0	0.16	SiP_2O_7
Si $2p_{1/2}$					104.6	0.08	

NMR spectra were recorded by using a Bruker AVIII spectrometer (400 MHz for ^{1}H). ^{1}H chemical shifts in are referenced to internal tetramethylsilane. Characterization data of benzodiazepines **1** and **5** are in good agreement with those previously reported using other catalytic systems [17,18].

Compound **6** (mixture of isomers A and B, ratio: 1:1): ^{1}H NMR (400 MHz, [D_6]DMSO):δ 6.92–6.89 (2H, m), 6.85 (1H, d), 6.81–6.78 (1H, m), 6.76 (1H, d), 6.73–6.71 (1H, m), 2.20 (3H, s), 2.18 (3H, s), 2.17 (2H, s), 2.12 (2H, s), 1.23 (6H, s), 1.22 (6H, s), 1.21 (18H, s). ^{13}C NMR (400 MHz, [D_6]DMSO):δ 170.98, 169.85 (C═N), 148.3142.62,139.36, 139.24, 137.29, 136.32, 127.64, 124.09, 122.39, 121.09, 117.76, 116,93 (aromatics), 67.03, 65.42 (C-N), 46.24, 45.79 (CH_2), 34.39, 34.04 (C-CH_3), 31.81, 31.70 (^{t}Bu), 30.55, 30.50 (CH_3), 29.98, 29.88 (CH_3).

2.4. Theoretical calculations

Theoretical calculations were performed with the Gaussian 09 software package [19]. Geometries were optimized using RB3LYP/6–31 +G (d,p). The stationary points were characterized by means of harmonic vibrational frequency analysis. Thus, the transition structures were confirmed to be first-order saddle points. The imaginary frequency was inspected in each to ensure it represented the desired reaction coordinate. For key transition states, the intrinsic reaction coordinate (IRC) was followed to ensure it connects the reactants and products.

3. Results and discussion

3.1. Characterization of carbon materials

Carbon catalysts have been synthesized by pyrolysis of tires followed by activation with CO_2 or H_3PO_4 or not. Char yield for the pyrolysis assays was 37.9 % after hexane extraction. It was observed an increase in ash content of the obtained carbon materials due to the concentration effect of pyrolysis, reaching 21.3 % in the case of the CPN_H_3PO_4 activated with acid. Elemental analysis demonstrates that the chars have high carbon content as well as sulphur, 86.7 % and 2.67 % respectively (Table 1).

The char presented a pH_{PZC} value of 6.80, indicating an almost neutral surface, while CPN_H_3PO_4 presents an acid surface, as expected (Table 1).

TGA curves depicted in Fig. 1a showed that mass loss of 70 % for ST rubber occurs up to around 440 °C. It was observed that from this temperature the thermal degradation was stabilized, remaining around 30 % of carbonaceous residue. The char still loses around 18 % of its mass up to 900 °C, indicating the presence of some unconverted carbon. However, all ACs showed high thermal stability, loosing small amount of mass but only at higher temperatures.

Mineral analysis of CPN confirmed the higher content in zinc and silicon among the other metals and metalloids [5]. This is an expected result because both zinc and silica are present in the tire manufacturing process.

In addition, peaks observed in the XRD analysis of the char CPN and CPN_CO_2 are mainly attributed to zinc sulfide (ZnS). Interestingly there is no significant difference between these two samples, indicating that the CO_2 treatment may have been insufficient to introduce relevant transformations. However, the CPN_CO_2 catalyst revealed an increase in the pH_{pzc} (Table 1) indicating some possible modification in more liable surface chemical groups.

In the case of CPN_H_3PO_4 the XRD pattern is totally different probably due to the presence of phosphate species (Fig. 1b). In fact, the diffractogram of sample activated with H_3PO_4 reveals the disappearance of zinc-derived peaks and there is the appearance of new peaks mainly associated with the silicophosphate (SiP_2O_7) phase due to the reaction of amorphous silica with H_3PO_4 [20]. Probably the activation with phosphoric acid, followed by intense washing resulted in the solubilization of the zinc and consequent leaching from the sample. However, new functional groups could have been introduced in the materials surface as revealed by the XRD. The silica present in the rubber as a consequence of the tire manufacturing process, is retained in the carbonaceous material recovered after the rubber pyrolysis, even after chemical activation with phosphoric acid, where as a result of this acid activation there is the appearance of new functional groups, namely silicophosphate.

The morphology of the samples and qualitative composition was analyzed by scanning electron microscopy coupled with EDS analysis (Fig. 2). The results supported the observations made for the XRD results. Samples CPN and CPN_CO_2 revealed an unequivocally presence of zinc in the surface, that can be identified in the image and was confirmed

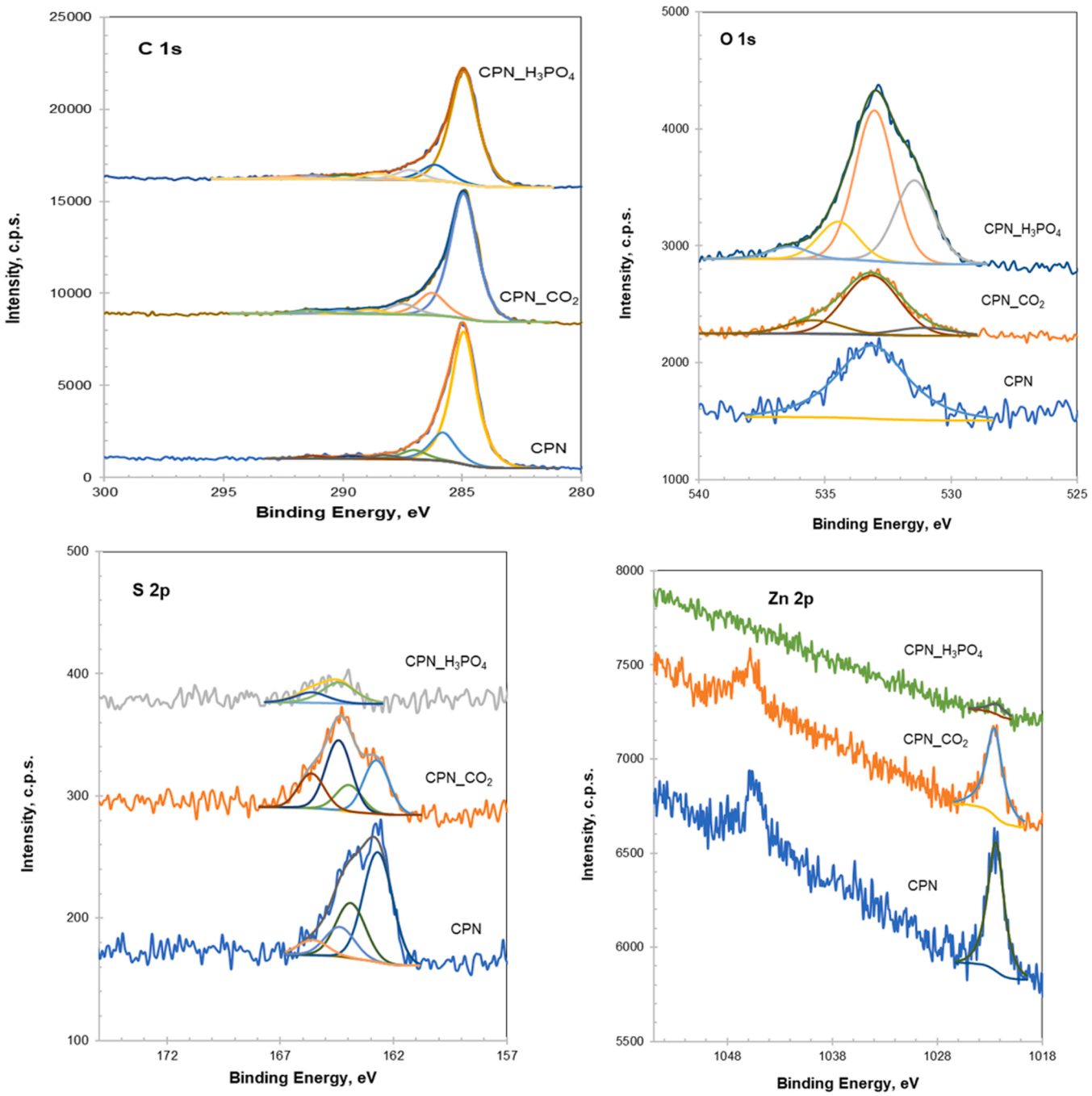

Fig. 3. XPS detailed regions C 1 s, O 1 s, S 2p and Zn 2p for the three samples CPN, CPN_CO_2 and CPN_H_3PO_4.

by the EDS analysis. Additionally, the SEM images of this samples revealed that the morphology of the material did not change much, probably the activation time under CO_2 stream was not enough to introduce major defects in the material surface even if some increase in porosity is observed.

On the other hand, the sample activated with phosphoric acid seems denser and the EDS could not identify the presence of any zinc phase. These are heterogeneous materials and, in some areas, (the darker areas of the image) it could be identified P and C indicating the possible formation of phosphates in the carbon surface, while in lighter areas of the material it could be identified Si and P in greater relative amount. These observations supported the XRD result where no crystalline form of Zn was detected, and the observed peak pattern can be attributed to silicophosphate.

Samples were also analysed by XPS. The elements carbon, oxygen, sulphur, silicon, zinc, phosphorus and nitrogen were studied through the XPS regions C 1 s, O 1 s, S 2p, Si 2p, Zn 2p, P 2p and N 1 s. The global quantification is presented in Table 2a and the detailed quantification, together with the chemical assignments, in Table 2b. Fig. 3 presents XPS spectra with the respective fittings for the main regions.

C 1 s region was fitted with 6 components (except for the CPN_H_3PO_4 where 7 components were needed) constrained to have the same full width at half maximum and the same Gaussian-Lorentzian mixture. No attempt was done for distinguishing between the sp^3 and sp^2 contribution. The first three components include both contributions as well as the asymmetry typical of the graphitic component. The two last components are assigned to $\pi \rightarrow \pi^*$ transitions. The intermediary peaks correspond to carbons bonded to oxygen. The oxygen region presents a

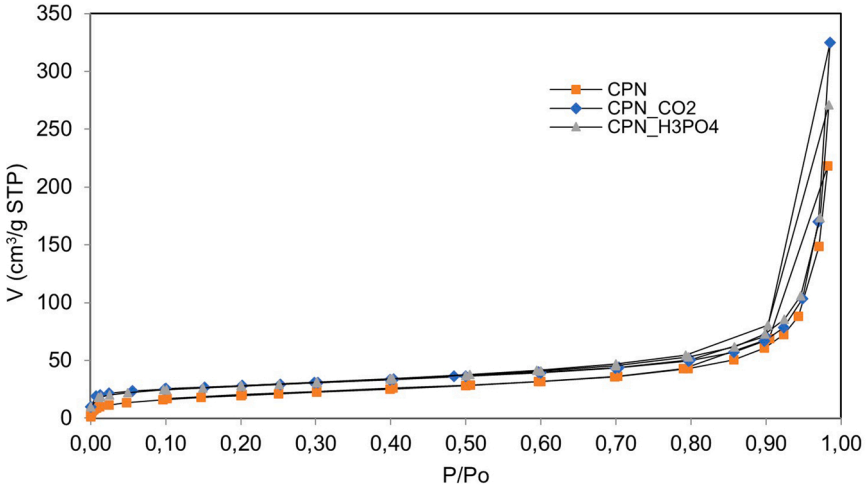

Fig. 4. N_2 adsorption-desorption isotherm of (a) CPN and (b) CPN_CO_2 and (c) CPN_H_3PO_4 at 77 K. samples.

Table 3
Textural parameters of carbon samples.

	S_{BET} (m^2/g)	V_{total} (cm^3/g)	V_{micro} (cm^3/g)	V_{meso} (cm^3/g)
CPN	69	0.14	0.01	0.13
CPN_CO_2	95	0.14	0.02	0.12
CPN_H_3PO_4	48	0.11	0.004	0.11

very structured envelope for the CPN_H_3PO_4 sample contrarily to the two first ones, CPN and CPN_CO_2, which present a broad band centered at 533.1 ± 0.1 eV. This oxygen in higher relative amount for the CPN_H_3PO_4 sample is essentially bound to carbon surface comprising phosphate groups and silicophosphate phase, whereas in the case of CPN and CPN_CO_2 samples, it is probably bonded to zinc. Particularly interesting are the peaks at 287.2 eV (**C 1s**) [21] and 531.5 eV (**O 1s**), in the carbon and oxygen regions, assigned to -O-PO_3H_2 species anchored to the carbon surface (C-O-PO_3H_2) [22]. As it can be seen in Tables 2a 2b, sulphur and nitrogen are also present in all the samples, nitrogen being detected as traces. CPN and CPN_CO_2 samples showed the presence of S^{2-} ion, likely in the form of ZnS (S $2p_{3/2}$, centered at 162.7 ± 0.1 eV), as well as the presence of the thiol function, C-S-H (the main component centered at 164.4 ± 0.1 eV) [23]. For CPN_H_3PO_4 sample just the thiol form is detected, in accordance with the XRD results. Note that although zinc was found as Zn^{2+} species in investigated samples, the amount was notably diminished for CPN_H_3PO_4 (around 1/10 of the amount found in the other samples). Finally, silicon and phosphorus are just found in the sample CPN_H_3PO_4. Considering the amounts, silicon exists just in the form of SiP_2O_7 as demonstrated by XRD. However, the amount of phosphorus exceeds the stoichiometric one, strongly suggesting that it exists also in the form of C-OPO_3H_2 as shown at carbon and oxygen regions.

The N_2 adsorption-desorption isotherms, at 77 K, of samples as well as the textural parameters obtained from those are presented in Fig. 4 and Table 3, respectively.

All the samples showed very similar adsorption isotherm with a profile typical of non-porous or macroporous materials, a type II isotherms according to the IUPAC classification. The obtained hysteresis loop is type H3, and these are typical of tire derived chars (Fig. 4) and similar to other reported in the literature [24]. In this sense, all the samples presented lower S_{BET} ranging 95–48 m^2/g, and a very similar V_{meso}. Sample CPN_CO_2 presented a slight increase in surface area but no significant change in other textural parameters.

FTIR spectra for all the samples are very similar; in the case of the sample activated with acid, CPN_H_3PO_4, it was also observed a new band at 1035 cm^{-1} and a group of small bands between 750 and 650 cm^{-1} which can be associated with PO-Si, Si-O-Si or P-O-P vibrations (Fig. 5), indicating the presence of acid phosphorous groups in the carbon surface.

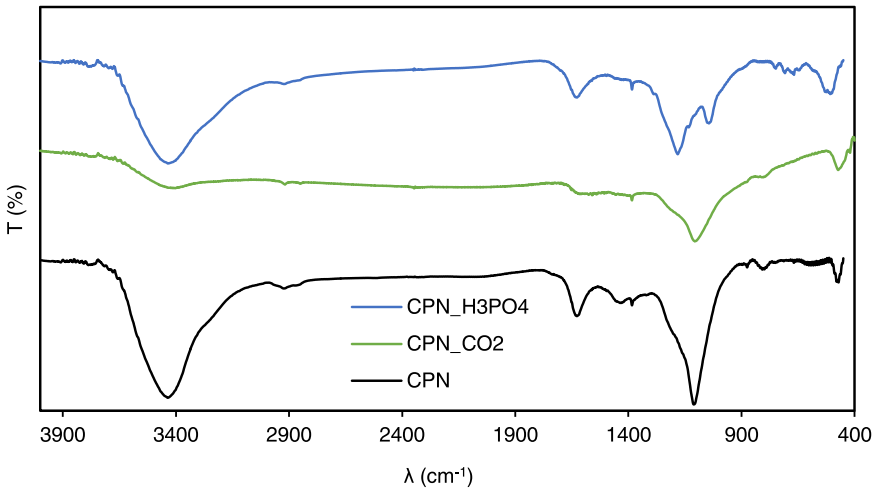

Fig. 5. FTIR of carbon-based materials.

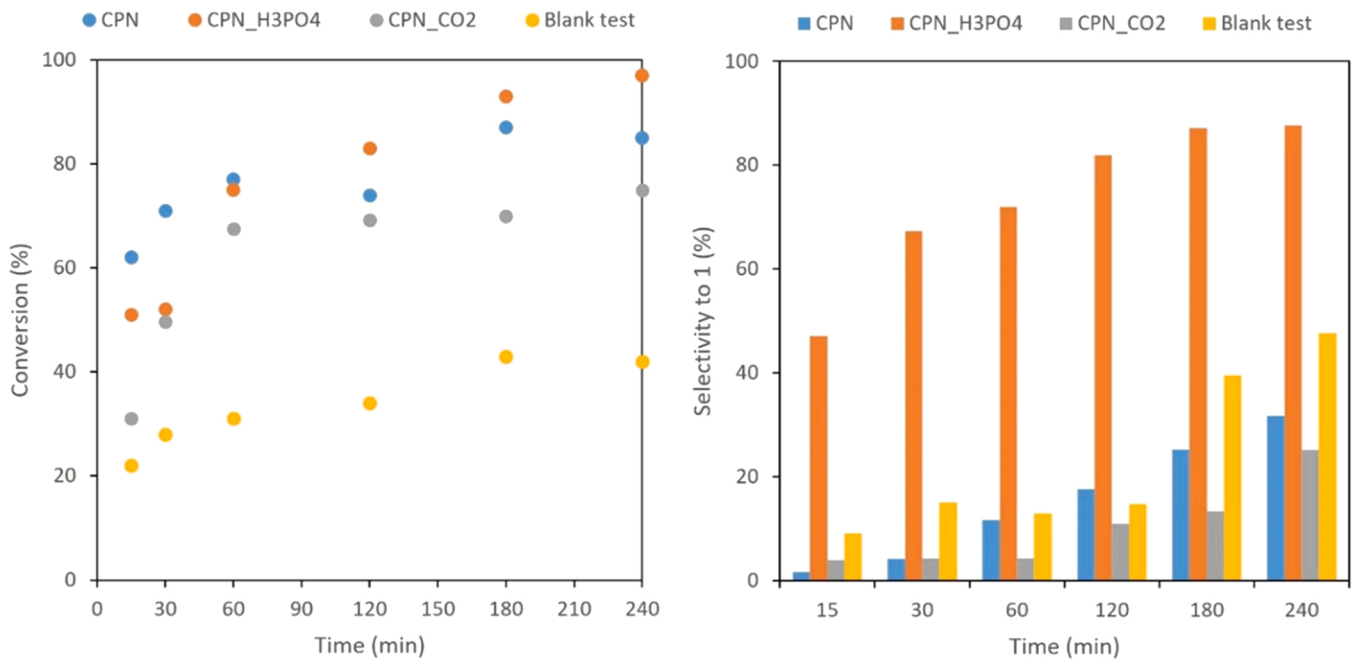

Fig. 6. Synthesis of 2,2,4-trimethyl-2,3-dihydro-1*H*-1,5-benzodiazepine **1** from *o*-phenylendiamine **2** and acetone **3**, at 50 ºC (catalyst amount: 50 mg).

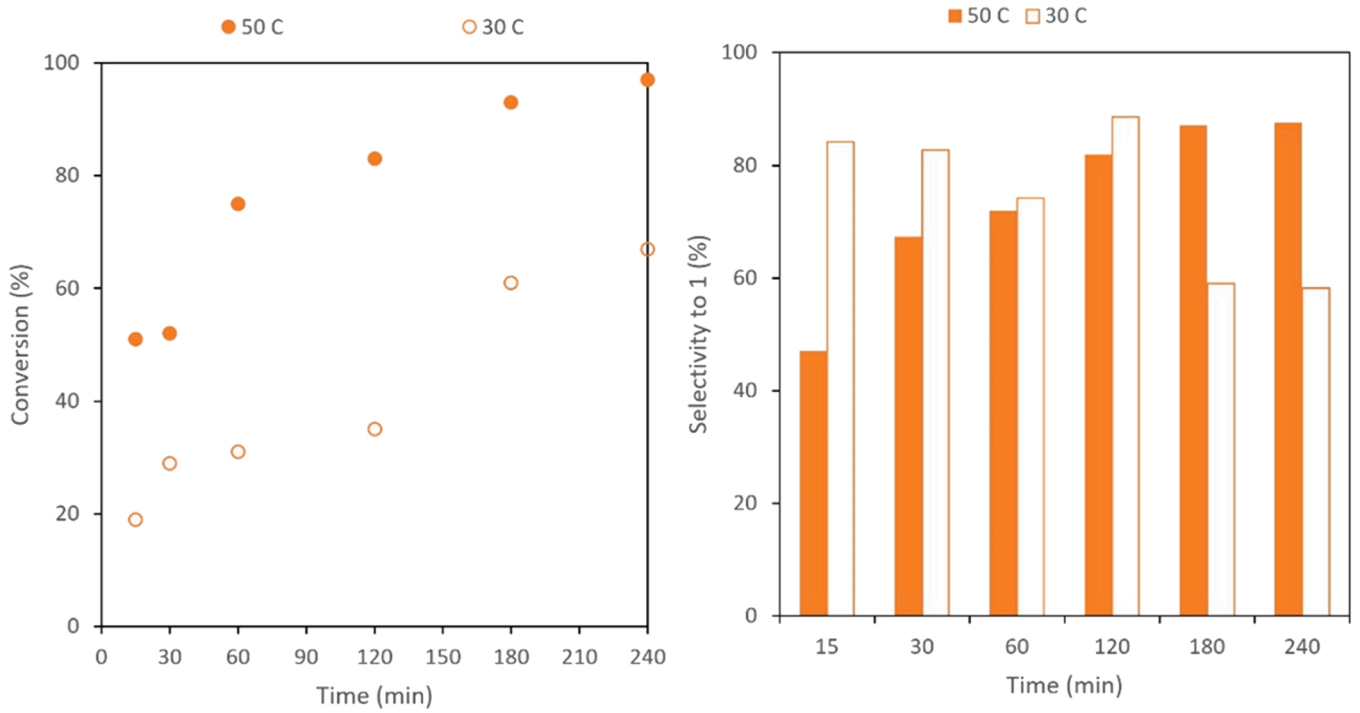

Fig. 7. Influence of temperature into the synthesis of 2,2,4-trimethyl-2,3-dihydro-1*H*-1,5-benzodiazepine **1** from *o*-phenylendiamine **2** and acetone **3**, in the presence of CPN_H_3PO_4 catalyst (catalyst amount: 50 mg).

3.2. *Catalytic performance*

Carbon materials under study were firstly tested in the synthesis of 2,2,4-trimethyl-2,3-dihydro-1*H*-1,5-benzodiazepine **1** from *o*-phenylendiamine **2** in the presence of acetone **3** excess, at 50 ºC (Scheme 1).

Investigated carbons gave rise to conversions of around 80 % in just 1 h of reaction time, becoming almost quantitative conversion after 4 h when using CPN_H_3PO_4 (Fig. 6). However, important differences were observed concerning selectivity towards the formation of the corresponding benzodiazepine **1**, being close to 90 % in the presence of CPN_H_3PO_4 sample (Fig. 6). It is well-known that 1*H*-1,5-benzodiazepines are formed following the sequence double imination reaction between diamine and ketones, imine-enamine tautomerization and final cyclization reaction. During the reaction in the presence of CPN catalysts it was observed the formation of an intermediate compound, identified as 2,2-dimethyl-2,3-dihydro-1*H*-benzo[*d*]imidazole **4** (Scheme 1), which evolve slowly to the desired benzodiazepine **1** [11]. The fact that selectivity to **1** was increased with the reaction time is in accordance

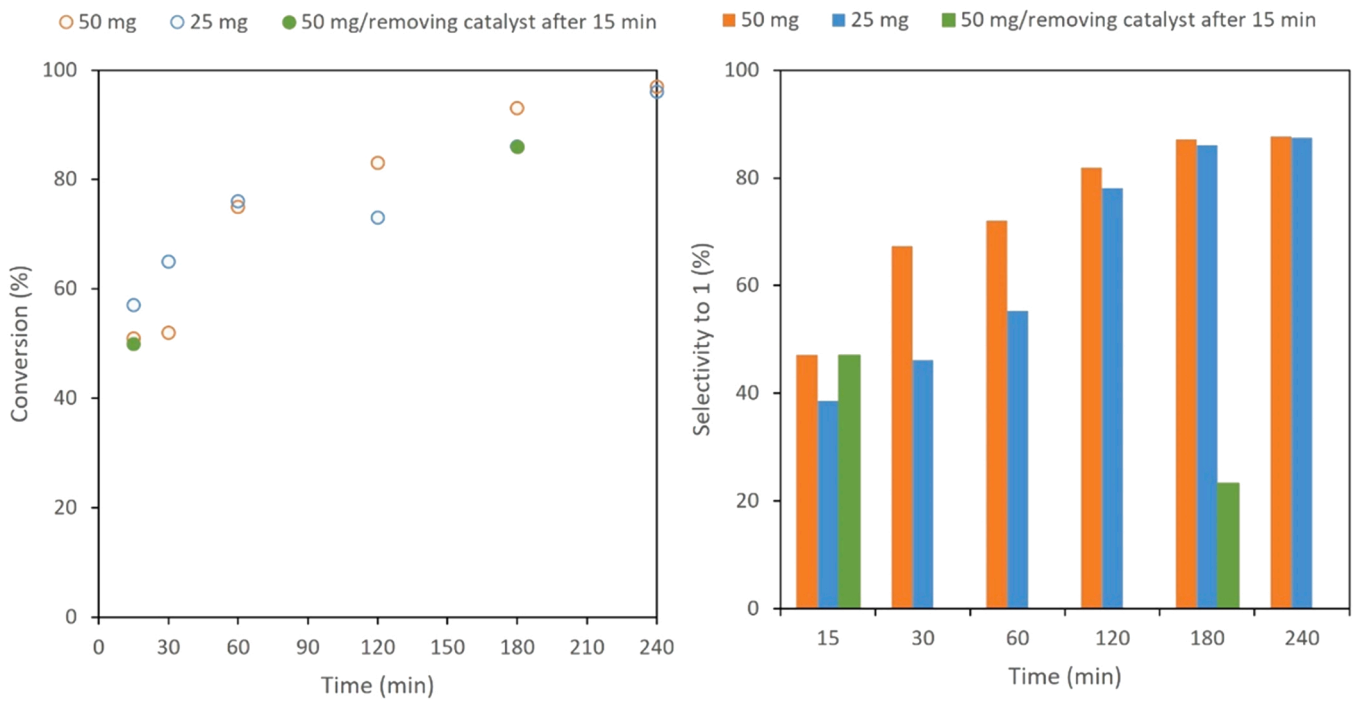

Fig. 8. Influence of catalyst amount into the synthesis of 2,2,4-trimethyl-2,3-dihydro-1*H*-1,5-benzodiazepine **1** from *o*-phenylendiamine **2** and acetone **3**, at 50 °C, in the presence of CPN_H_3PO_4 catalyst.

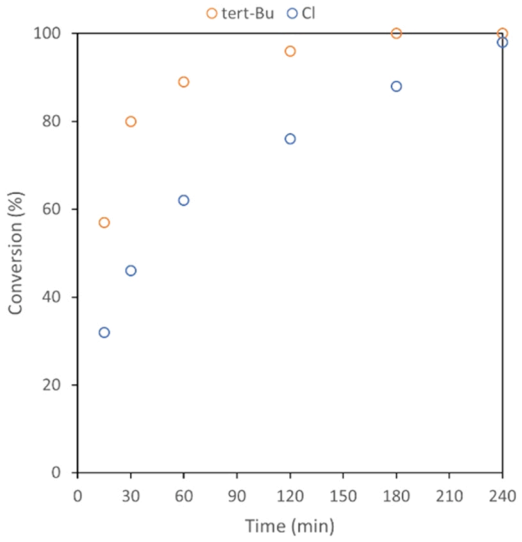

Fig. 9. Synthesis of 7 or 8-substituted benzodiazepines **5** and **6** from 4-subtituted *o*-phenylendiamines **7** and **8** and acetone **3**, at 50 ºC, in the presence of CPN_H_3PO_4 catalyst (50 mg).

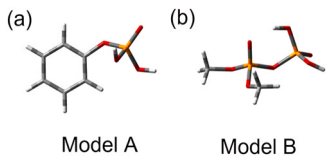

Fig. 10. Reduced models of active centers in CPN_H_3PO_4 catalyst. (a) C_6H_5-O-P = $O(OH)_2$ (Model A) (b) $Me_2P_2O_7H_2$ (Model B).

with a multistep synthesis, a valuable information concerning the reaction mechanism. In this context, since the most selective catalyst was the most acidic one, CPN_H_3PO_4, exhibiting a pH_{PZC} of 2.8 (Table 1), this result strongly suggests that last steps of the synthesis are mainly promoted under acidic conditions. Note that a blank experiment without catalyst, was carried out, under the same experimental conditions, affording 2,2,4-trimethyl-2,3-dihydro-1*H*-1,5-benzodiazepine **1** with 34 % of conversion and 15 % of selectivity, after 2 h of reaction time, conversion increasing to 42 % with 48 % of selectivity to **1** (4 h) (Fig. 6). Remarkably, selectivity to **1** was notably enhanced in the presence of CPN_H_3PO_4 catalyst, therefore, it seems that the observed reactivity is mainly governed by the chemical surface. Interestingly, CPN_H_3PO_4 catalyst can be reused during 2 consecutive cycles without catalytic activity loss maintaining both conversions and selectivity.

In addition, the reaction takes place even at low temperature, 30 °C, in the presence of CPN_H_3PO_4 catalyst, although with decreased conversion, as expected (Fig. 7). In this case, while selectivity to **1**, at 50 ºC, was increased with the time (up to 85 % after 3 h), at lower temperature, it was observed selectivity variations in such a manner that when the conversion is increased the selectivity decreases. This feature could indicate that the last step of the reaction comprising the cyclization would be favoured at higher temperatures, in this case 50 °C.

We also analysed the influence of the catalyst amount when using the CPN_H_3PO_4 sample as the most efficient catalyst, at 50 °C (Fig. 8).

The use of higher catalyst amount (50 mg) did not reach notably conversion differences, although selectivity to **1** was considerably increased, at the shortest reaction times. In both cases, 2,2,4-trimethyl-2,3-dihydro-1*H*-1,5-benzodiazepine **1** was yielded in 96 % with 90 % of selectivity, indicating that the optimized catalyst amount could be 25 mg.

We also carried out an experiment in the presence of CPN_H_3PO_4 sample (50 mg), at 50 °C, removing the catalyst after 15 min of reaction time and maintaining the reaction mixture under stirring during 3 h, at the same temperature (Fig. 8). We can observe that while the total conversion was increased to 86 %, the selectivity values to **1** was strongly diminished to 23 %, probably indicating, by one side, that no leaching of catalytic species was produced and, secondly, that the first

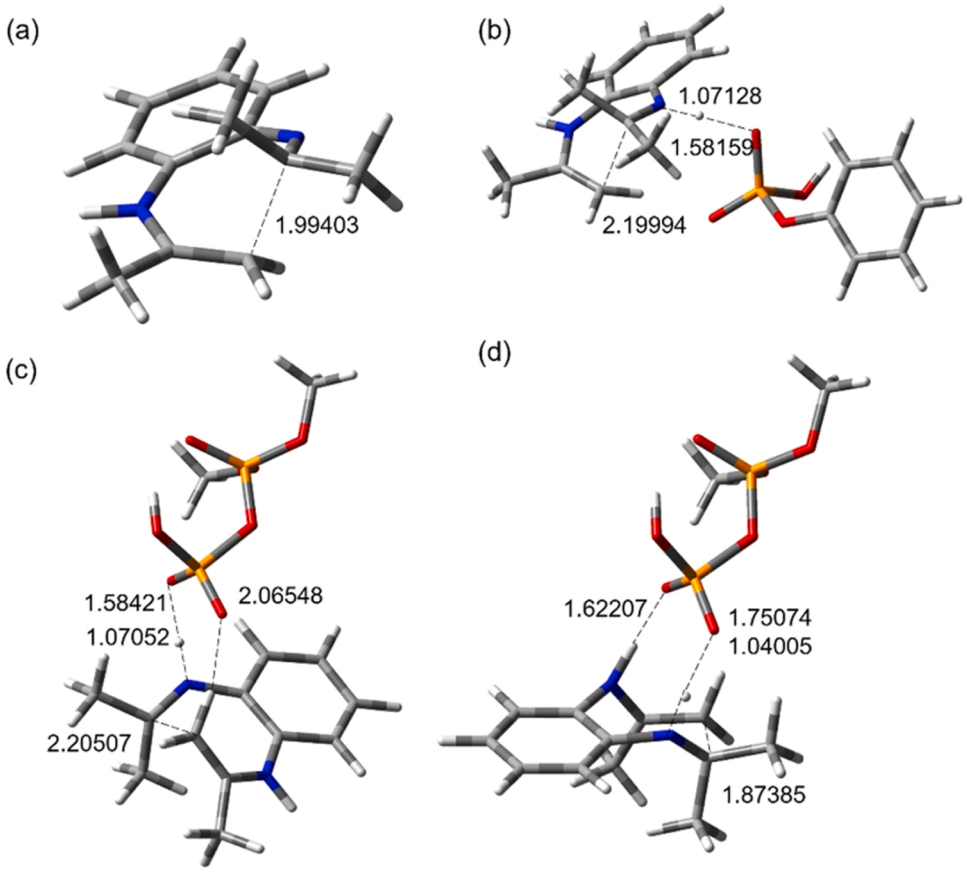

Fig. 11. Optimized transition structures for the cyclization step in the synthesis of benzodiazepines **1**. (a) Without catalyst, TS (b) in the presence of Model A, TS-A (c) in the presence of Model B, TS-B_1. (d) in the presence of Model B, TS-B_2. Relevant distances are expressed in Å.

Table 4
Gibbs Free energy and NPA charges computed for transition structures.

Transition Structure	ΔG (kcal/mol)	C-C distance (Å)	NPA[a]
TS	52.1	1.99403	0.322
TS-A	42.3	2.19994	0.384
TS-B_1	41.8	2.20507	0.376

DFT RB3LYP, 6–31 G+ (d,p). [a]NPA charges (Natural Population Analysis) in reactant complexes for C acceptor (C═N).

imination reactions could take place in absence of any catalyst but the acid catalysts was key for the final cyclization step to **1**.

Finally, we synthesize the substituted benzodiazepines **5** and **6**, in the presence of the most active and selective catalyst, CPN_H_3PO_4, from substituted *o*-phenylendiamines **7** and **8** and acetone **3**, under the same experimental conditions (Scheme 2).

In both cases, it was possible to selectively obtain the benzodiazepines **5 and 6** in almost quantitative yields, after 4 h of reaction time, as mixtures of the corresponding isomers A/B in a ratio 1:1 (Fig. 9). The obtained results indicate that the presence of *tert*-Bu moiety at position 4- in diamines **8**, as electrondonor substituent, notably increased the conversion values, probably due to the increase of the nucleophility of the amino functions. Contrarily, conversion was considerably diminished in the presence of electrowithdrawing substituent, in this case a chlorine atom. Remarkably, the corresponding benzodiazepines **5** and **6** were obtained with total selectivity.

3.3. Computational study

In addition, we carried out a computational study which could indicate the most probable catalytic specie in CPN_H_3PO_4 sample. Based on previous studies [25,26] and considering the composition and acidity of this sample, we selected the most reduced models (Fig. 10) simulating the catalytic active centers in the most effective catalyst, CPN_H_3PO_4. Model A comprises acidic phosphate functions (C-O-PO_3H_2) over the catalyst surface whereas Model B would represent a part of SiP_2O_7 phase. SiP_2O_7 is constituted by octahedral SiO_6 bound to pyrophosphate units. Considering that CPN_H_3PO_4 catalyst is a non-porous sample, acid centers in SiP_2O_7 could be constituted by acidic protons in pyrophosphate units at the edges. It is important to note that available Gaussian software does not allow to parametrize octahedral silicon, for this reason two positions in pyrophosphoric acid are blocked by methyl groups instead Si, then decreasing the computational cost.

Optimized transition structures (TS) in the presence of both models but also that in absence of any catalyst are shown in Fig. 11. It can be observed that TS is a more advanced transition structure than those containing both possible catalytic species, since the C-C bond distance is significantly smaller in TS than TS-A or TS-B_1 – 1.99403 Å (TS) *vs* 2.19994 Å (TS-A) and 2.20507 Å (TS-B_1) (Fig. 11a-c) – .

However, the ΔG for TS is almost 10 Kcal mol^{-1} higher than those observed for TS-A (42.3 Kcal mol^{-1}) or TS-B_1 (41.8 Kcal mol^{-1}) (Table 4). In the same context, energy activation barrier is notably superior for TS than TS-A or TS-B_1, up to 23 kcal mol^{-1} and, therefore, the reaction rate is increased in the presence of both models. It is important to note that in the case of Model B, it was observed a strong hydrogen bond between terminal OH and vicinal P = O (d P = O···H-O = 1.93970 Å) also formed in bare model. Nevertheless, we also found additional transition structures showing other interaction modes with selected models. Such is the case of TS-B_2 (Fig. 11d) in which it was observed the almost total transference of acidic proton in catalyst to basic nitrogen in C═N moiety, beside a strong hydrogen bond between

N-H and vicinal P = O. Both interactions strongly constrain the transition structure shortening the C-C distance to 1.87385 Å in TS-B_2 (Fig. 11d) and 1.88023 Å in TS-A_2 (not shown). Considering only the C-C distances for both it seems that the most probable transitions structures would be these last, TS-A_2 and TS-B_2. However, although the formation of the corresponding reactant complexes is energetically favored, the free energy barrier is up to 6 kcal mol^{-1} regarding TS-A or TS-B_1. Considering that the real catalyst is macroporous sample, the obtained results seem to indicate that the operative transition structures are those depicted in Fig. 11b and c.

In addition, we also calculated the NPA charges, based onto the Natural Population Analysis, for C acceptor (C═N), for the corresponding reactant complexes (Table 4). The slightly increased electrophilicity of C═N acceptor found for reactant complex derived from Model A is in accordance with the slightly reduced C-C distance in TS-A. Although the computed ΔG for both transition structures, TS-A or TS-B_1, are very close (42.3 *vs* 41.8 kcal mol^{-1}), the smallest ΔG found for TS-B_1 would suggest that this model could be behind of the observed reactivity.

Finally, combination of both experimental and theoretical results seems to indicate that the most probable catalytic active center could be that represented by the reduced Model B through TS-B_1 (Fig. 11c) and, therefore, by phosphate species from SiP_2O_7 phase, although the contribution of phosphate groups at the carbon surfaces *via* TS-A (Model A) cannot be neglected.

4. Conclusions

In summary, we report herein, for the first time, a type of carbonaceous materials prepared from tires which can efficiently catalyse the synthesis of benzodiazepines **1**, with high conversions and selectivity, under mild reaction conditions.

CPN and CPN_CO_2 catalysts afforded high conversion values (up to 70 % after 3 h), selectivity to **1** being lower than 30 %, indicating that carbon matrix is also involved in the first steps of the reaction consisting of the imination reactions. It is supported by the formation of intermediate specie **4** (Scheme 1) detected when using CPN and CPN_CO_2 samples as the main reaction product.

The most acidic sample, CPN_H_3PO_4, was found to be the most efficient catalyst leading to conversion values higher than 90 %, after 4 h of reaction time, selectively leading to 2,2,4-trimethyl-2,3-dihydro-1*H*-1,5-benzodiazepine **1** (90 %), which makes it a good alternative to other catalysts based on carbon materials previously reported [9,10]. Therefore, it seems that the observed reactivity is mainly governed by the chemical surface, specifically by the presence of acid functions as phosphate groups at carbon surface or supported SiP_2O_7 phase.

In addition, we also carried out a theoretical study, by computational methods, analyzing the last step of the reaction comprising the cyclization step. The combination of experimental and theoretical results strongly suggest that the most probable active specie could consist of phosphate functions in SiP_2O_7. Although the electrophilicity of carbon acceptor (C═N moiety) involved in cyclization step in the presence of both models are very close, the computed free energies would suggest that the model B could be act as preferred active site.

CRediT authorship contribution statement

Marina Godino-Ojer: Investigation; Writing - Original Draft. **Vanessa Ripoll Morales:** Investigation. **Antonio J. López Peinado:** Writing- Reviewing and Editing. **Maria Bernardo:** Writing- Reviewing and Editing. **Nuno Lapa:** Writing- Reviewing and Editing. **Ana Maria Ferraria:** Investigation; Writing- Reviewing and Editing. **Ana Maria Botelho do Rego:** Writing- Reviewing and Editing. **Isabel M. Fonseca:** Writing- Reviewing and Editing. **Ines Matos:** Conceptualization, Methodology, Writing- Reviewing and Editing. **Elena Pérez-Mayoral:** Conceptualization, Methodology, Writing- Reviewing and Editing, supervision.

Declaration of Competing Interest

The authors declare that they have no known competing financial interests or personal relationships that could have appeared to influence the work reported in this paper.

Data Availability

Data will be made available on request.

Acknowledgements

This work has been supported by Universidad Nacional de Educación a Distancia - UNED, Spain (project UNED 2021, NANOPORIM Ref. 096-034247), Francisco de Vitoria University, Spain (Project Ref. UFV2021-21) and the Associate Laboratory for Green Chemistry - LAQV which is financed by national funds from Fundação para a Ciência e a Tecnologia - FCT/MCTES, Portugal (UIDB/50006/2020). The Research Unit Institute for Bioengineering and Biosciences – iBB and the Associate Laboratory Institute for Health and Bioeconomy - i4HB were funded by Fundação para a Ciência e a Tecnologia - FCT/MCTES, Portugal through the projects UIDB/04565/2020 and UIDP/04565/2020, and LA/P/0140/2020. A.M. F. wishes to thank Instituto Superior Técnico for Scientific Employment contract IST-ID/131/2018. The authors also thank Valorpneu S.A. for the INOV.AÇÃO 2018 Award.

References

[1] https://www.etrma.org/, s.f.
[2] E.L.K. Mui, D.C.K. Ko, G. McKay, Production of active carbons from waste tyres—a review, Carbon 42 (2004) 2789–2805, https://doi.org/10.1016/j.carbon.2004.06.023.
[3] I. Jones, M. Zhu, J. Zhang, Z. Zhang, J. Preciado-Hernandez, J. Gao, D. Zhang, The application of spent tyre activated carbons as low-cost environmental pollution adsorbents: a technical review, J. Clean. Prod. 312 (2021), 127566, https://doi.org/10.1016/j.jclepro.2021.127566.
[4] K. Frikha, L. Limousy, J. Pons Claret, C. Vaulot, K. Florencio Pérez, B. Corzo Garcia, S. Bennici, Potential valorization of waste tires as activated carbon-based adsorbent for organic contaminants removal, Materials 15 (2022) 1099, https://doi.org/10.3390/ma15031099.
[5] M. Nogueira, I. Matos, M. Bernardo, F. Pinto, N. Lapa, E. Surra, I. Fonseca, Char from spent tire rubber: a potential adsorbent of remazol yellow dye, C. — J. Carbon Res. 5 (2019) 76, https://doi.org/10.3390/c5040076.
[6] A.S. Al-Rahbi, P.T. Williams, Production of activated carbons from waste tyres for low temperature NOx control, Waste Manag. 49 (2016) 188–195, https://doi.org/10.1016/j.wasman.2016.01.030.
[7] J.B. Bariwal, K.D. Upadhyay, A.T. Manvar, J.C. Trivedi, J.S. Singh, K.S. Jain, A. K. Shah, 1,5-Benzothiazepine, a versatile pharmacophore: a review, Eur. J. Med. Chem. 43 (2008) 2279–2290, https://doi.org/10.1016/j.ejmech.2008.05.035.
[8] R.K. Singh, S. Sharma, A. Kaur, M. Saini, S. Kumar, Current development in multicomponent catalytic synthesis of 1,5-benzodiazepines: a systematic review, Iran. J. Catal. 6 (2016) 1–22.
[9] R. Mishra, A.K. Sharma, R. Kumar, V. Baweja, P. Mothsra, M.K. Singh, S.B. Yadav, Solid support based synthesis of 1,5-benzodiazepines: a mini review, Synth. Commun. 52 (2022) 481–503, https://doi.org/10.1080/00397911.2021.2024855.
[10] M. Godino-Ojer, L. Milla-Diez, I. Matos, C.J. Durán-Valle, M. Bernardo, I. M. Fonseca, E. Pérez Mayoral, Enhanced catalytic properties of carbon supported zirconia and sulfated zirconia for the green synthesis of benzodiazepines, ChemCatChem 10 (2018) 5215–5223, https://doi.org/10.1002/cctc.201801274.
[11] M. Godino-Ojer, I. Matos, M. Bernardo, R. Carvalho, O.S.G.P. Soares, C. Durán-Valle, I.M. Fonseca, E. Pérez Mayoral, Acidic porous carbons involved in the green and selective synthesis of benzodiazepines, Catal. Today 357 (2020) 64–73, https://doi.org/10.1016/j.cattod.2019.11.027.
[12] P.O. Ibeh, F.J. García-Mateos, R. Ruiz-Rosas, J.M. Rosas, J. Rodríguez-Mirasol, T. Cordero, Acid mesoporous carbon monoliths from lignocellulosic biomass waste for methanol dehydration, Materials 12 (2019) 2394–24080, https://doi.org/10.3390/ma12152394.
[13] F.J. García-Mateos, R. Ruiz-Rosas, J.M. Rosas, J. Rodríguez-Mirasol, T. Cordero, Phosphorus containing carbon (submicron)fibers as efficient acid catalysts, Catal. Today 383 (2022) 308–319, https://doi.org/10.1016/j.cattod.2020.10.025.
[14] M.J. Valero-Romero, E.M. Calvo-Muñoz, R. Ruiz-Rosas, J. Rodríguez-Mirasol, T. Cordero, Phosphorus-containing mesoporous carbon acid catalyst for methanol dehydration to dimethyl ether, Ind. Eng. Chem. Res 58 (2019) 4042–4053, https://doi.org/10.1021/acs.iecr.8b05897.

[15] I. Matos, M.F. Silva, R. Ruiz-Rosas, J. Vital, J. Rodríguez-Mirasol, T. Cordero, J. E. Castanheiro, I.M. Fonseca, Methoxylation of α-pinene over mesoporous carbons and microporous carbons: a comparative study, Microporous Mesoporous Mater. 199 (2014) 66–73, https://doi.org/10.1016/j.micromeso.2014.08.006.
[16] M.A. Montes-Morán, D. Suárez, J. Angel Menéndez, E. Fuente, The basicity of carbons, in: Novel Carbon Adsorbents, Elsevier Ltd, 2012, pp. 173–203, https://doi.org/10.1016/B978-0-08-097744-7.00006-5.
[17] M. Jeganathan, K. Pitchumani, Solvent-free syntheses of 1,5-benzodiazepines using HY zeolite as a green solid acid catalyst, ACS Sustain. Chem. Eng. 2 (2014) 1169–1176, https://doi.org/10.1021/sc400560v.
[18] J.S. Yadav, B.V.S. Reddy, S. Praveenkumar, K. Nagaiah, Indium(III) bromide: a novel and efficient reagent for the rapid synthesis of 1,5-benzodiazepines under solvent-free conditions, Synthesis 3 (2005) 0480–0484, https://doi.org/10.1002/chin.200529176.
[19] Frisch, M.J., Trucks, G.W., Schlegel, H.B., Scuseria, G.E., Robb, M.A., Cheeseman, J.R., Scalmani, G., Barone, V., Mennucci, B., Petersson, G.A., Nakatsuji, H., Caricato, M., Li, X., Hratchian, H.P., Izmaylov, A.F., Bloino, J., Zheng, G., Sonnenberg, J.L., Had, M., Gaussian 09, Revision C.01, Gaussian, Inc., Wallingford CT, 2010 (n.d.).
[20] M. Khabbouchi, K. Hosni, M. Mezni, E. Srasra, Simplified synthesis of silicophosphate materials using an activated metakaolin as a natural source of active silica, Appl. Clay Sci. 158 (2018) 169–176, https://doi.org/10.1016/j.clay.2018.03.027.
[21] K.S. Siow, L. Britcher, S. Kumar, H.J. Griesser, XPS study of sulfur and phosphorus compounds with different oxidation states, Sains Malays. 47 (2018) 1913–1922, https://doi.org/10.17576/jsm-2018-4708-33.
[22] J. Bedia, R. Ruiz-Rosas, J. Rodríguez-Mirasol, T. Cordero, Kinetic study of the decomposition of 2-butanol on carbon-based acid catalyst, AIChE J. 56 (2010) 1557–1568, https://doi.org/10.1002/aic.12056.
[23] [NIST X-ray Photoelectron Spectroscopy Database. NIST Standard Reference Database 20, Version 4.1. Data compiled and evaluated by Alexander V. Naumkin, Anna Kraut-Vass, Stephen W. Gaarenstroom, and Cedric J. Powell, 2012. Available online: https://srdata.nist.gov/xps/. https://doi.org/10.18434/T4T88K].
[24] M. Betancur, C.N. Arenas, J.D. Martínez, M.V. Navarro, R. Murillo, CO_2 gasification of char derived from waste tire pyrolysis: Kinetic models comparison, Fuel 273 (2020), 117745, https://doi.org/10.1016/j.fuel.2020.117745.
[25] J. López-Sanz, E. Pérez-Mayoral, E. Soriano, D. Omenat-Morán, C.J. Durán, R. M. Martín-Aranda, I. Matos, I. Fonseca, Acid-activated carbon materials: cheaper alternative catalysts for the synthesis of substituted quinolines, ChemCatChem 5 (2013) 3736–3742, https://doi.org/10.1002/cctc.201300626.
[26] M. Godino-Ojer, R. Blazquez-García, I. Matos, M. Bernardo, I.M. Fonseca, E. Pérez Mayoral, Porous carbons-derived from vegetal biomass in the synthesis of quinoxalines, Mech. Insights Catal. Today 354 (2020) 90–99, https://doi.org/10.1016/j.cattod.2019.06.043.